Ordered Au/Pb nanoring arrays on Pb-induced Si(111)-1×1 surface

Lin Tang,[1] Ze-Lei Guan,[1] Dan Hao,[2] Xu-Cun Ma,[1] Jin-Feng Jia,[2,a)] and Qi-Kun Xue[1,2,a)]
[1]*Institute of Physics, Chinese Academy of Sciences, Beijing 100190, People's Republic of China*
[2]*Department of Physics, Tsinghua University, Beijing 100084, People's Republic of China*

(Received 27 December 2008; accepted 22 January 2009; published online 11 February 2009)

Growth and morphology of Au on a homogenous Si(111)-1×1-Pb surface are investigated using scanning tunneling microscopy. The deposited Au atoms grow on the Si(111)-1×1-Pb surface in two-dimensional mode and a long-range ordered 8×8 reconstruction with ringlike structure is observed following room temperature deposition. Upon thermal annealing to 500 K, the 8×8 structure transforms into a hexagonal-ring array with a 4×4 superstructure. The mechanism for the formation of the two self-organized nanostructures is discussed in terms of interface diffusion, alloying, and energy minimization. © *2009 American Institute of Physics*.
[DOI: 10.1063/1.3081017]

Metal nanostructures with a periodic alignment have attracted a considerable amount of attention[1–6] due to their potential technological applications in optoelectronics,[7] microelectronics,[8] and magnetic data storage.[9,10] As a common phenomenon in multimetallic systems, spontaneous alloying of binary metals can lead to the formation of well-ordered two-dimensional (2D) nanostructures on semiconductor substrates. Extensive investigations of the atomic scale structures of either Pb or Au overlayer on Si(111) have been widely carried out.[11–17] By depositing submonolayer coverages of Pb on a Si(111) surface, several reconstructions have been reported to form γ-$\sqrt{3}\times\sqrt{3}$, β-$\sqrt{3}\times\sqrt{3}$, 1×1, and α-$\sqrt{3}\times\sqrt{3}$ with either hexagonal incommensurate (HIC) or stripe incommensurate structure.[11–14] In the case of Au, in addition to the common α-$\sqrt{3}\times\sqrt{3}$ and β-$\sqrt{3}\times\sqrt{3}$ phases, 5×2 and 6×6 can also be formed depending on the Au coverage and the substrate temperature.[15–17] Relatively little information is available on the formation of 2D ordered structure of Au/Pb surface alloys on Si(111) although various forms of Au/Pb alloys have been observed to form when Pb is deposited onto a gold substrate.[18–20] In this letter, we report for the first time that depositing submonolayer of Au on a homogenous Si(111)-1×1-Pb surface gives rise to various superstructures upon thermal annealing. Two highly regular nanoring arrays of Si(111)-8×8-Au/Pb and Si(111)-4×4-Au/Pb can be produced through metal alloying. The alloying process is strongly influenced by the presence of the silicon substrate, leading to the formation of a 2D Au/Pb alloy with unique structures and 2D ordering.

All experiments were performed in an ultrahigh vacuum system equipped with a variable-temperature scanning tunneling microscope (Omicron VT-STM). The clean 7×7 reconstructed Si(111) (*n*-type with a resistivity of 2–3 Ω cm, 0.05°) was prepared following the standard high-temperature flashing procedures.[1] About 1.0 ML Pb [1 ML=the surface atomic density in the topmost layer of the unreconstructed Si (111) surface] was deposited at a flux of 0.25 ML/min from a pyrolytic boron nitride crucible onto the Si(111)-7×7 substrate at room temperature (RT). Thermal annealing of the sample at 550 K for a few seconds and subsequent cooling down to RT resulted in an atomically flat Si(111)-1×1-Pb structure.[11] Au was then evaporated onto the 1×1-Pb surface from a Knudsen cell held at 1380 K with a calibrated deposition rate of 0.07 ML/min. All the STM images were recorded at RT.

The Si(111)-1×1-Pb is selected as the substrate instead of the γ-Pb/Si(111) and β-Pb/Si(111) phases due to its homogeneity.[11–13] Furthermore, the 1×1-Pb has a Pb surface coverage of 1 ML and is thus more effective in shielding the deposited Au atoms from the substrate silicon atoms because all the dangling bonds on the Si surface are saturated by Pb atoms.[11]

Figure 1(a) displays a typical STM topographic image after 0.05 ML of Au was deposited onto the Si(111)-1×1-Pb surface at RT. 2D islands are observed on the terraces of the substrate and in Fig. 1(a) about 5% (±1%) of the substrate is covered by the 2D islands. The top surface of the islands displays an ordered lattice structure consisting of a regular array of nanorings, as shown in Fig. 1(b). The 2D nanoring lattice constant is measured to be 3.1 nm along each principle axis. This is eight times of the surface lattice constant for the Si(111) surface (3.84 Å). Therefore, this superstructure has a (8×8) periodicity with the long diagonal along the $[\bar{1}\bar{1}2]$ direction, which does not belong to either Au- or Pb-induced reconstructions on Si(111). According to the corresponding height histogram, Fig. 1(c), the island marked as B in Fig. 1(a) is 2.29 Å high as measured from the Si(111)-1×1-Pb substrate (marked as A), which is lower than the monolayer height for either Au (2.36 Å) or Pb (2.86 Å). Therefore we propose that the 2D islands formed upon deposition of Au onto the Si(111)-1×1-Pb substrate are of 2D Au/Pb alloy. Silicon atoms are unlikely to be incorporated into the surface alloy because too much energy would be required to break the Si–Si back bonds. The silicon substrate, however, does influence the structure of the Au/Pb alloy as evidenced from the (8×8) geometry, which is clearly linked to the underlying substrate.

With about 5% of the surface covered by the 2D Au/Pb alloy islands, the rest of the Si(111)-1×1-Pb substrate retains its initial surface structure. A high-resolution STM image of the Si(111)-1×1-Pb substrate shown in Fig. 1(d) shows both the Pb atoms (brighter spots) in the topmost layer and the underlying Si atoms (the less bright spots). The unit

a)Authors to whom correspondence should be addressed. Electronic addresses: jjf@mail.tsinghua.edu.cn and qkxue@mail.tsinghua.edu.cn.

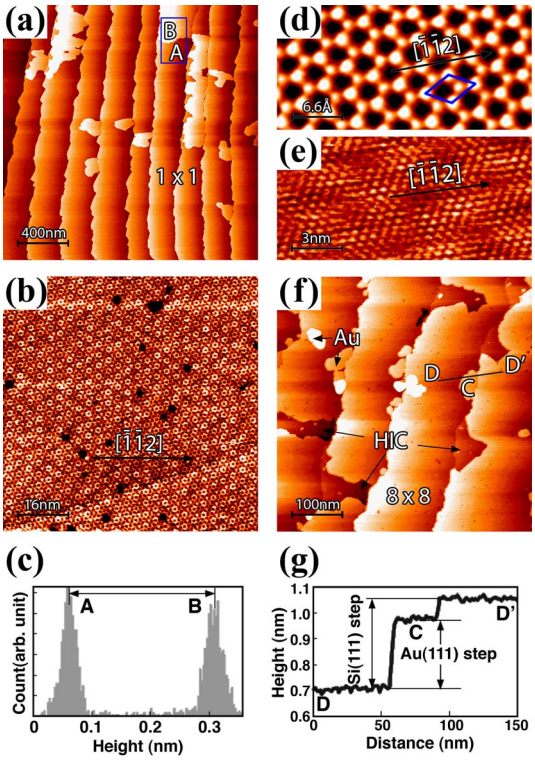

FIG. 1. (Color online) STM images recorded at a sample bias $V_s=-2$ V and a tunneling current $I=0.02$ nA for different coverages of Au grown on the Si(111)-1×1-Pb substrate. (a) 0.05 ML Au deposited at RT. The Si(111)-1×1-Pb substrate and the coexisting Au/Pb overlayer are marked by "A" and "B," respectively. (b) The zoomed-in STM image ($V_s=0.2$ V, $I=0.02$ nA) of the 8×8-Au/Pb island in the region marked B in (a). (c) The histogram of height distribution showing the height difference of the 1×1-Pb substrate and the Au/Pb overlayer in (a). (d) STM image ($V_s=-2$ mV, $I=0.1$ nA) showing the well-ordered honeycomb structure of the Si(111)-1×1-Pb surface in region A. (e) STM image ($V_s=+0.7$ V, $I=0.02$ nA) showing the structure of a transition phase from the 1×1 to the HIC-Pb phase after 0.25 ML Au deposition on the 1×1-Pb surface at RT. (f) Image of the surface following 0.65 ML Au deposited at RT. (g) The height profile along the line DD′ marked in (f).

cell consisting of one Pb atom and one Si atom, corresponding to an overall 1 ML coverage, is outlined by a blue parallelogram. As more Au atoms are deposited onto the surface, the 2D alloy islands increase in size. By the time the coverage reaches 0.25 ML, a HIC phase, Fig. 1(e), appears in the vicinity of the 8×8-Au/Pb islands. In comparison with previous studies,[14,21,22] this new phase is identified as the HIC-Pb/Si(111) phase corresponding to a Pb coverage of 1.2–1.33 ML. The appearance of the HIC-Pb/Si(111) phase next to the 8×8-Au/Pb islands suggests that during the alloying process, some Pb atoms are released and pushed to the boundaries of the alloy island. These Pb atoms are subsequently incorporated into the Si(111)-1×1-Pb structure leading to the formation of the higher Pb coverage HIC-Pb/Si(111) phase.

When an equivalent of 0.65 ML of Au is deposited onto the surface, the 8×8-Au/Pb islands cover most of the substrate and the remaining exposed Pb/Si(111) substrate is completely transformed into the HIC-Pb phase, Fig. 1(f). Moreover, some isolated flat-top small islands (one marked as C) occur on top of the first Au/Pb adlayer. Using line profiles such as the one shown in Fig. 1(g), the height of these islands measures 2.37 Å, which is nearly equal to a gold monatomic layer height (2.36 Å). The growth of these

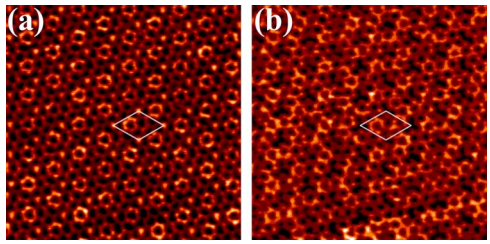

FIG. 2. (Color online) STM images of the 8×8-Au/Pb structure obtained with (a) $V_s=0.35$ V and (b) $V_s=-0.35$ V. The two images (25×25 nm^2) are acquired from the same region. The parallelograms indicate the 8×8 unit cell.

islands scales with the amount of gold deposited onto the 2D surface, and thus the bright islands sitting on top of the alloy phase are assumed to be gold islands. Due to the Ehrlich–Schwoebel barrier, Au atoms prefer to nucleate at the step edges, and as a result most of the gold islands are found to be attached to step edges.

In order to obtain more detailed structural information about the Au/Pb surface alloy, high resolution imaging was performed and the resulting images from the Si(111)-8×8-Au/Pb region are shown in Figs. 2(a) and 2(b). These images were obtained at RT with the sample bias voltages of 0.35 and −0.35 V, respectively. It can be clearly seen that the apparent surface structure depends on the bias polarity. In the empty-state image, Fig. 2(a), the Si(111)-8×8-Au/Pb superstructure appears periodic with a complicated unit cell consisting of a hexagonal ring, a Y-shaped structure, and a bright dot. In a more detailed view, the dot is actually a triangular protrusion. However, the filled-state image, Fig. 2(b), looks less uniform in height with some hexagonal rings appearing more elevated than others, and the Y-shaped structures not as obvious as those in Fig. 2(a). The triangular protrusions in Fig. 2(a) appear as depressions in Fig. 2(b). On the other hand, the surface morphology on a larger scale is very flat at both polarities. The root mean square of the height deviation is only 0.1 Å. Although a structural model for the supercell of the 8×8-Au/Pb alloy is unknown at this stage, the inhomogeneous features in the high resolution images and the long-ranged ordering of the 8×8 phase clearly indicate that it is a surface alloy with a Pb–Au ratio of ~1.

The 8×8-Au/Pb alloy phase can also be obtained by deposition of Au onto Si(111)-1×1-Pb below RT (~150 K). The growth of the Au/Pb overlayer follows a perfect 2D mode. At a coverage of 1 ML, the substrate terraces can be totally covered by the 8×8-Au/Pb layer. Assuming that there is no Pb desorption from the surface at this temperature, the experiment further suggests that the Pb/Au ratio in 8×8 is nearly one. However, in comparison with the structure prepared at RT, the Au/Pb layer prepared at 150 K possesses more domains, and even after annealing to RT the Au/Pb structure is still less uniform due to kinetically limited interface diffusion (not shown). Therefore, the degree of order is dominantly determined by interface diffusion and alloying. When Au is deposited at RT, an enhanced thermal diffusion can promote the intermixing between the Pb and Au atoms and thus a more uniform layer is formed.

To further study the thermal response of the 8×8-Au/Pb, the sample with a RT 8×8-Au/Pb alloy layer was annealed up to 550 K *in situ*. Several new structures with different lattice constants and morphologies emerged

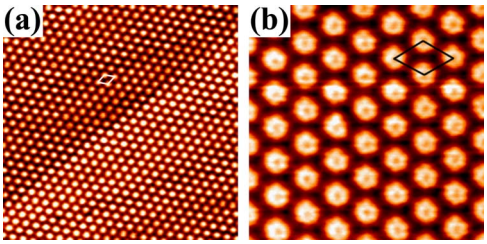

FIG. 3. (Color online) STM images of the well-ordered 4×4 superstructure. (a) Image size is 45×45 nm^2 and tunneling parameters are -0.6 V and 0.02 nA. (b) Zoomed-in (11×11 nm^2) image showing the ring feature of the surface obtained using -0.3 V and 0.02 nA.

during annealing. This result strongly suggests the occurrence of further alloying during the annealing process. It is interesting to note that a perfect nanodot array can be seen with a long-range order on the surface in Fig. 3(a) after the 8×8-Au/Pb sample with an initial Au coverage of 0.65 ML was annealed from RT to 500 K. High-resolution filled-state STM image, Fig. 3(b), reveals that each nanodot in Fig. 3(a) is actually a hexagonal ring. The distance between the centers of the neighboring rings is about 1.6 nm corresponding to approximately four times of the Si(111) lattice constant. Therefore the supercell indicated by the solid-line parallelograms in Figs. 3(a) and 3(b) has the same (4×4) periodicity with the long diagonals along the $[\bar{1}\bar{1}2]$ direction. No significant change is observed at different sample voltages, so the surface is metallic and the two images shown in Fig. 3 are occupied-state images.

The annealing process is likely to have induced the breaking of the Pb–Si bonds leading to the segregation of Pb atoms to the surface to form the observed nanorings. This conjecture is based on energy minimization because the surface free energy of Pb(0.5 J/m^2) is much lower than those of Au(1.6 J/m^2) and Si(1.2 J/m^2).[9] In addition, the Au–Si bond is much stronger (3.65 eV/bond) than the Pb–Si bond (2.65 eV/bond).[23,24] Thus under appropriate conditions, substitution of Pb atoms by Au atoms occurs and the surface alloy reorganizes into a well ordered array of nanorings. Considering the exchange process and increased Pb desorption at higher annealing temperature, the 4×4 phase might correspond to a surface alloy Au_2Pb, which is a thermodynamically stable bulk phase.[25] The perfection of the 4×4-(Au/Pb) surface suggests that it is a potentially useful template for the fabrication of nanoscale devices.

In summary, we have fabricated self-assembled ordered arrays of 8×8-Au/Pb and 4×4-Au/Pb superstructures utilizing interface diffusion, surface energy minimization, and surface alloying of Au and Pb. Their unique structures make these two nanoring arrays promising for various applications. For example, the reconstructed surface can serve as a template for the controlled positioning of other atomic or molecular superstructures. Thus the present investigation will pave the way for the fabrication of more complex nanoscale structures for novel devices.

The work was supported by the National Natural Science Foundation of China and the Ministry of Science and Technology of China. The authors thank Quanmin Guo for critical reading of the manuscript.

[1] J. L. Li, J. F. Jia, X. J. Liang, X. Liu, J. Z. Wang, Q. K. Xue, Z. Q. Li, J. S. Tse, Z. Zhang, and S. B. Zhang, Phys. Rev. Lett. **88**, 066101 (2002).
[2] J. F. Jia, J. Z. Wang, X. Liu, and Q. K. Xue, Appl. Phys. Lett. **80**, 3186 (2002).
[3] Y. P. Chiu, L. W. Huang, C. M. Wei, C. S. Chang, and T. T. Tsong, Phys. Rev. Lett. **97**, 165504 (2006).
[4] J. F. Jia, X. Liu, J.-Z. Wang, J. L. Li, X. S. Wang, Q. K. Xue, Z. Q. Li, Z. Zhang, and S. B. Zhang, Phys. Rev. B **66**, 165412 (2002).
[5] S. C. Li, J. F. Jia, R. F. Dou, Q. K. Xue, I. G. Batyrev, and S. B. Zhang, Phys. Rev. Lett. **93**, 116103 (2004).
[6] M. H. Pan, H. Liu, J. Z. Wang, J. F. Jia, Q. K. Xue, J. L. Li, S. Y. Qin, U. M. Mirsaidov, X. R. Wang, J. T. Market, Z. Zhang, and C. K. Shih, Nano Lett. **5**, 87 (2005).
[7] A. O. Orlov, I. Amlani, G. H. Bernstein, C. S. Lent, and G. L. Snider, Science **277**, 928 (1997).
[8] R. P. Andres, T. Bein, M. Dorogi, S. Feng, J. I. Henderson, C. P. Kubiak, W. Mahoney, R. G. Osifchin, and R. Reifenberger, Science **272**, 1323 (1996).
[9] F. J. Himpsel, J. E. Ortega, G. J. Mankey, and R. F. Willis, Adv. Phys. **47**, 511 (1998).
[10] S. Sun, C. B. Murray, D. Weller, L. Folks, and A. Moser, Science **287**, 1989 (2000).
[11] L. Tang, J. F. Jia, B. Sun, Z. L. Guan, D. Hao, P. Zhang, S. B. Zhang, and Q. K. Xue (unpublished).
[12] E. Ganz, I. S. Hwang, F. Xiong, S. K. Theiss, and J. Golovchenko, Surf. Sci. **257**, 259 (1991).
[13] J. M. Gómez-Rodríguez, J. Y. Veuillen, and R. C. Cinti, Surf. Sci. **377**, 45 (1997).
[14] S. Stepanovsky, M. Yakes, V. Yeh, M. Hupalo, and M. C. Tringides, Surf. Sci. **600**, 1417 (2006).
[15] S. Hasegawa, X. Tong, S. Takeda, N. Sato, and T. Nagao, Prog. Surf. Sci. **60**, 89 (1999).
[16] H. M. Zhang, T. Balasubramanian, and R. I. G. Uhrberg, Phys. Rev. B **65**, 035314 (2001).
[17] D. Grozea, E. Bengu, and L. D. Marks, Surf. Sci. **461**, 23 (2000).
[18] J. P. Biberian and G. E. Rhead, J. Phys. F: Met. Phys. **3**, 675 (1973).
[19] J. Perdereau, J. P. Biberian, and G. E. Rhead, J. Phys. F: Met. Phys. **4**, 798 (1974).
[20] U. Bardi, Rep. Prog. Phys. **57**, 939 (1994).
[21] K. Horikoshi, X. Tong, T. Nagao, and S. Hasegawa, Phys. Rev. B **60**, 13287 (1999).
[22] L. Seehofer, G. Falkenberg, D. Daboul, and R. L. Johnson, Phys. Rev. B **51**, 13503 (1995).
[23] G. LeLay, M. Manneville, and R. Kern, Surf. Sci. **65**, 261 (1977).
[24] M. Saitoh, K. Oura, K. Asano, F. Shoji, and T. Hanawa, Surf. Sci. **154**, 394 (1985).
[25] S. Hassam and Z. Bahari, J. Alloys Compd. **392**, 120 (2005).